ON THE DEVELOPMENT OF AN INTERIOR BALLISTIC MODEL FOR SMALL CALIBER ARMOR PIERCING AMMUNITION

Rotariu Adrian-Nicolae, Trana Eugen

Military Technical Academy Av. George Cosbuc 39-49, Bucharest, Romania
Fax: +32(0)2 7376352
E-mail: adrian.rotariu@mta.ro

Abstract: *A new analytic continuous function for nonlinear deterred/undeterred propellant transition is proposed. Using CEA software, variable ballistic characteristics are determined for a given propellant composition. Several modifications of the interior ballistic specific equations should be operated in order to deal with variability of mean values of burned propellant characteristics: impetus, specific heat at constant pressure, adiabatic coefficient, gas constant, covolume.*

Keywords*: interior ballistics; 0D model; deterred/undeterred transition;*

1. Introduction

A permanent goal of ballistics community is to develop mathematical models able to represent accurately the interior ballistic phenomena. Currently, there are used several types of such models. Most intensively used and also the first developed models are 0-dimensional (lumped) models, like those attributed to Corner [1] or Drozdov [2] or other more recently developed like STANAG 4367 model [3] or IHGBV2 code [4]. For a more detailed analysis of the interior ballistic phenomena, multidimensional models can be used [5].

The using of grains of variable composition like deterred grains imposes supplementary hypothesis on 0D models. Usually approach is to admit a very sharp transition of the propellant properties which allows treating the propellant charge as being made of two distinct compositions, each one with its own set of characteristics, that burn in a successive way. As long as the sharp transition is in fact only an hypothesis, the alternative approaches of gradual transition, as linear or multi-step transitions, were proposed for deterred grains [4, 6].

The present work deals with the necessary adjustments of a lumped model for small caliber grooved barrel to implement the true deterred/undeterred profile transition of grains.

2. Deterrent concentration profile function

Deterring along the complex geometry represent the most used ways to assure a progressive burning of propellant grains. The impregnation of grains exterior surface with substances like DNT or DBP will reduce the characteristic burning rate of propellant on the affected volume with significant consequence on the pressure time gradient recorded during ballistic cycle. As both deterrent concentration and impregnation depth are of importance for ballistic calculations, as work of Mann has already shows [7], the interest of researches on determination of such deterring characteristics is understandable. Along time several techniques, alone or in conjunction, like Fourier transform infrared (FTIR) microspectroscopy and laser Raman microspectroscopy [8] were used to measure the above mentioned characteristics. Depending on the type of deterrent diffusion mechanism, Fickcian or non-Fickcian and the composition and manufacturing process of grains, several types of deterred/undeterred profile were calculated or identified:

- a thick layer of constant or nearly constant deterrent concentration followed by a relatively thin region were the concentration fall to zero value (case I) [7,9]
- a thin layer of constant or nearly constant deterrent concentration followed by a thick region were the concentration fall to zero value (case II) [10]

- a continuous variation of deterrent concentration from the highest value at the exterior surface till the zero somewhere inside of the grain (case III - Fickian diffusion) [8]

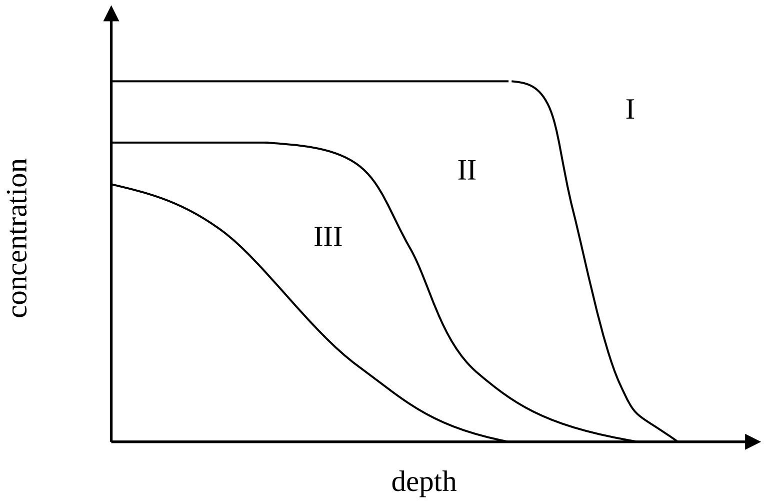

Fig. 1 The observed categories of deterrent concentration profiles

As can be seen in fig. 1, except the case I, none of the deterring profiles may be approximated in a satisfactory way with a sharp transition. As regarding the continuous functions able to describe such transitions, the following exponential analytical expression representing the solution of one-dimensional diffusion in anisotropic media when the diffusion is initiated by an instantaneous plane source was found to be well suited to several deterrent concentration profiles of case III [8].

$$c(r,t) = \frac{s}{\sqrt{\pi D t}} e^{-\frac{r^2}{4Dt}} \qquad (1)$$

where *c* is the deterrent concentration, *t* the diffusion time, *D* the constant diffusion coefficient, *s* is the surface concentration of deterrent and *r* the space coordinate.

As long as the function (1) is not able to model cases I and II, we identified another analytical function derived from the cumulative distribution function of Gumbel distribution, that admit an constant plateau followed by a decrease of similar shape to function (1):

$$c(r) = c_0 \left(1 - e^{-e^{-\frac{1}{\beta}(r-\mu)}}\right) \qquad (2)$$

where c_0 is the concentration of deterrent in the layer of constant concentration plateau , μ is the coefficient that controls the thickness of above mentioned layer and β is the coefficient that controls the thickness of layer of variable concentration. It is obvious that this formulation allow us to model all three identified cases from Fig.1 by variation of the μ and β values. In Fig. 2 we exemplify the ability of such function to approximate the concentration profile of a spherical single base deterred propellant measured by infrared (IR) microscopy which shows a thin layer of constant deterrent concentration followed by a thick region with variable concentration [10]. For extreme high values of β the proposed function became a step function of very sharp transition.

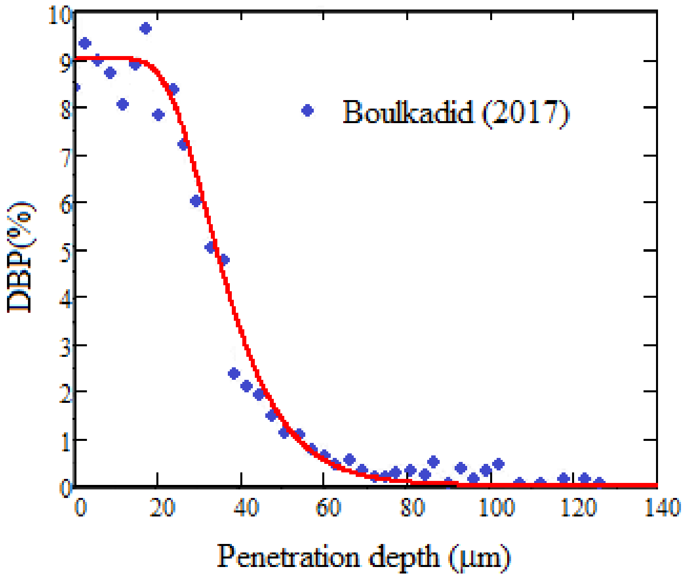

Fig. 2 The profile of function (2) for $c_0 = 9; \beta = 10; \mu = 32$ against the experimental data provided by Boulkadid [10] for DBP concentration in a spherical single base propellant

3. Influence of deterrent concentration on the propellant properties

As is wide know, the deterrent presence has an influence on all relevant propellant ballistic characteristics, each characteristic varying from y_d, the value specific to maximum concentration of deterrent to y_u, the value specific to undeterred propellant. Establishing the deterrent concentration profile law, $c(r)$, and assuming an known variation of the characteristic, $y(c)$, allow us to find the $y(r)$ relationship between an characteristic and the burning surface position r. If it assumes that the $y(c)$ relationship is monotonic one, e. g the impetus decreases as the concentration of deterrent increases, we may use the polynomial function

$$y(r) = y_u - (y_u - y_d)\left(\frac{c(r)}{c_0}\right)^n = y_u - (y_u - y_d)\left(1 - e^{-e^{-\frac{1}{\beta}(r-\mu)}}\right)^n \qquad (3)$$

where the index n allows the description on nonlinear relationship.

In the development of our ballistic model we have considered the relation (3) in order to describe the variation of flame temperature T_1, impetus f, covolume α, adiabatic coefficient γ and propellant density ρ . Beside those above mentioned characteristics the modification of the burning rate coefficients a and ν from the Saint Robert's relationship $\frac{dr}{dt} = ap^{\nu}$ is expected too. The Saint Robert's expression became

$$\frac{dr}{dt} = a(r)\, p^{\nu(r)} \qquad (4)$$

where $a(r)$ and $\nu(r)$ functions can expressed by (3) or another relationship type.

For the present case study we considered the spherical propellant analyzed by Boulkadid [10], with the deterred/undeterred transition profile given in Fig.1, used in experimental shooting tests with 5.56 mm EPVAT barrel. In order to establish the propellant characteristics variation, namely isochoric flame temperature T_1, impetus f, covolume α and adiabatic coefficient γ we have utilized NASA CEA thermochemical equilibrium [12].

In the absence of any other relevant information about the distribution of all others propellant ingredients along the radius of the propellant grain in question we consider that relative ratio of such ingredients remain unchanged. By doing so, having the propellant ingredients global concentrations given by Boulkadid [10], we were able to calculate the propellant ingredients local concentrations for different DPB concentrations. The results for six different DBP concentrations are listed in Tabel 1.

Tabel 1. Concentrations values of ingredients as function of DBP concentration

Substance	Concentrations (%)						
	Global value	for 9% DBP	for 7% DBP	for 5% DBP	for 3% DBP	for 1% DBP	for 0% DBP
NC	81.52	77.92	79.64	81.35	83.06	84.77	85.63
H2O	0.66	0.63	0.64	0.66	0.67	0.69	0.69
KNO3	1.2	1.15	1.17	1.20	1.22	1.25	1.26
NGL	10.7	10.23	10.45	10.68	10.90	11.13	11.24
DBP	4.8	9.00	7.00	5.00	3.00	1.00	0.00
DPA	0.59	0.56	0.58	0.59	0.60	0.61	0.62
NDPA	0.53	0.51	0.52	0.53	0.54	0.55	0.56
Total	100	100.00	100.00	100.00	100.00	100.00	100.00

For each such compositions the isochoric flame temperature T_1, impetus f, and adiabatic coefficient γ were directly calculated with CEA software for an initial temperature of 21°C, a load density of 0.2 g/cc and a NC nitration of 13.16%. The covolume α was determined with the approximation formula

$\alpha \cong 0.001 w_1$ (5)

where specific volume w_1 was determined with CEA software in the same conditions. The calculated values for each compositions of Tabel 1 are listed in Tabel 2. The influence of deterrent concentration on characteristics values are shown in a normalized way in Fig 3. The index power n of (3) formula for each characteristic is given in the last line of Table 2.

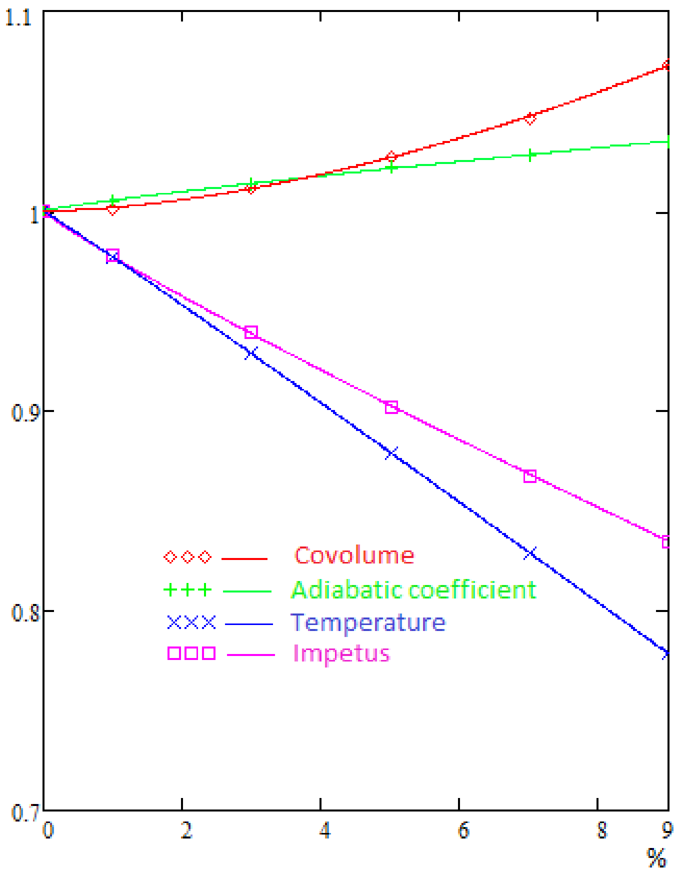

Fig. 3. Relative variations of propellant characteristics as functions of DBP concentration

Tabel 2. Characteristics values for different DBP concentrations

	Impetus [MJ/kg]	Isochoric flame temperature [°K]	Adiabatic coefficient	Covolume [m³/kg]
0%DBP	1.151	3368	1.200	0.000931
1%DBP	1.126	3290	1.206	0.000932
3%DBP	1.081	3127	1.216	0.000942
5%DBP	1.038	2960	1.226	0.000956
7%DBP	0.998	2791	1.234	0.000974
9%DBP	0.961	2622	1.242	0.000999
Index coeff.	0.9	1.03	0.85	1.7

4. Development of 0D model for small caliber grooved barrel with continuous nonlinear deterrent/undeterred transition

Other several modifications are necessary in the equations where the variable propellant characteristics are present. Firstly, the expression of mean pressure p, derived from energy conservation principle, used to calculate the burning rate will be

$$p = \frac{\int_0^r f(r)\frac{d\omega_b}{dr}dr - \left(\frac{\int_0^r \gamma(r)\frac{d\omega_b}{dr}dr}{\omega_b} - 1\right)\left(\frac{\varphi q v^2}{2} + E\right)}{W_0 + sx - \frac{\omega}{\delta_m}(1-\psi) - \int_0^r \alpha(r)\frac{d\omega_b}{dr}dr}, \qquad (6)$$

where ω is total mass of propellant, ω_b burned mass of propellant, ψ volume fraction of burned propellant, q projectile mass, v projectile velocity, φ supra-unitary coefficient used to taking account the secondary losses proportional to projectile kinetic energy $\frac{qv^2}{2}$, E secondary losses not proportional to projectile kinetic energy, W_0 initial volume of cartridge, s barrel cross section area, x space traveled by projectile inside of barrel and δ_m mean solid propellant density. Denominator expression $W_0 + sx - \frac{\omega}{\delta_m}(1-\psi) - \int_0^r \alpha(r)\frac{\omega_b}{dr}dr$ represent the volume behind projectile available for propellant gasses W.

Secondly, using propellant variable ballistic characteristics imposes an amendment of mean temperature equation, which became in the absence of terms related to igniter contribution

$$T_g = \frac{pW}{\int_0^r \frac{f(r)}{T_1(r)}\frac{\omega_b}{dr}dr}, \qquad (7)$$

where $\frac{1}{\omega_b}\int_0^r \frac{f(r)}{T_1(r)}\frac{\omega_b}{dr}dr$ is the gas constant for the ω_b burned propellant.

Also, the variable propellant characteristics affect the heat transferred to the barrel from the hot gasses. This secondary loss is calculated based on the heat transfer rate equation used in STANAG 4367, which became

$$\frac{dQ}{dt} = \left[\lambda\left(\int_0^r \frac{f(r)\gamma(r)}{T_1(r)(\gamma(r)-1)}\frac{d\omega_b}{dr}dr \frac{1}{W + \int_0^r \alpha(r)\frac{d\omega_b}{dr}dr}\frac{v}{2}\right) + \alpha_0'\right]\cdot S(x)\left(T_g - T_p\right) \qquad (8)$$

where $\frac{1}{\omega_b}\int_0^r \frac{f(r)\gamma(r)}{T_1(r)(\gamma(r)-1)}\frac{\omega_b}{dr}dr$ is specific heat at constant pressure of the ω_b burned propellant.

The heat loss rate depends on the difference between gas temperature T_g and wall temperature T_p, the dimension of exposed surface $S(x)$ and the thermal transfer coefficient, last term being the first parenthesis of the (7) equation right member. The Nordheim friction factor λ of thermal transfer coefficient depends on the barrel caliber D_t and α_0' is the natural convection coefficient.

Finally, the link between ω_b burned mass of propellant and the ψ volume fraction of burned propellant is given by

$$\omega_b = \frac{\omega}{\rho_m}\int_0^r \rho(r)\frac{d\psi}{dr}dr = \frac{\omega}{\rho_m}\int_0^r \rho(r)\frac{\chi}{r_1}\left(1 + 2\lambda\frac{r}{r_1} + 3\mu\left(\frac{r}{r_1}\right)^2\right)dr \qquad (9)$$

where r_1 correspond to a complete burning of propellant charge and χ, λ and μ. are shape coefficients used by Serebriakov [11].

5. Conclusions

Based on previous considerations, the following conclusions can be drawn:

- analytical function derived from the cumulative distribution function of Gumbel distribution can model successfully all identified types of deterred/undeterred profiles trough variation of the specific μ and β parameters
- except the burning rate coefficients a and ν from the Saint Robert's relationship and local density the others specific propellant characteristics can be calculated based on thermochemical equilibrium algorithms like those used in NASA CEA software
- the adaptation of an lumped interior ballistic model to an continuous nonlinear deterred/undeterred profile consists in modifying several equations to account variability of mean values of burned propellant impetus, specific heat at constant pressure, adiabatic coefficient, gas constant, covolume, density and Saint Robert's law parameters.

Acknowledgment

This work was carried out through the PN III Program 1 Development of national research system - carried out with the support of MEN, UEFISCDI project no. 20PCCDI/2018.

References:

1. Corner J., Theory of Interior Ballistics of Guns. New York, 1950, John Wiley & Sons.
2. Serebryakov M., Internal Ballistics (in Russian), 1949, Moscow: Oborongiz.
3. STANAG 4367 Land (Edition 3). 2012. THERMODYNAMIC INTERIOR BALLISTIC MODEL WITH GLOBAL PARAMETERS, Military Agency for Standardization, Brussels.
4. Anderson R.D., Fickie D.K., IBHVG2 – A User Guide, BRL-TR-2829, Ballistic Research Laboratory, 1987
5. Carlucci E. D., Sidney S. J., Ballistics. Theory and Design of Guns and Ammunition (second edition), 2014, Boca Raton, FL: CRC Press Taylor & Francis Group.
6. Albert W. H. and Michael J. N., The Influence of Propellant Deterrent Concentration Profile on Interior Ballistics Predictions Using Lumped-Parameter and Multiphase Flow Codes, ARL-TR-4713, 2009
7. D. C. Mann, DEVELOPMENT OF A DETERRED PROPELLANT FOR A LARGE CALIBER WEAPON SYSTEM, Journal of Hazardous Materials, vol. 7, 1988, pp.259-280
8. Vogelsanger B., Ossola B., Bronnimann E., The Diffusion of Deterrents into Propellants Observed by FTIR Microspectroscopy - Quantification of the Diffusion Process, Propellants Explos. Pyrotech, vol. 21, 1996, pp. 330-336
9. Trewartha S., Shapter J., Gibson C. T., Mikajlo E., Jones A., Determination of Deterrent Profiles in Nitrocellulose Propellant Grains Using Confocal Raman Microscopy, Propellants Explos. Pyrotech., vol. 36, 2011, pp. 451 – 458
10. Boulkadid K. M., Lefebvre M. H., Jeunieau L., Dejeaifve A., Local Temperature Sensitivity Coefficients of a Deterred Spherical Single Base Gun Propellant, Cent. Eur. J. Energ. Mater. vol. 14, 2017, pp. 952-965
11. Serebriakov, M. E., Interior Ballistics of Tube Weapons and Solid Propellant Rocket, Moskva, 1962

www.grc.nasa.gov/WWW/CEAWeb/ceaguiDownload-win.htm